International Journal of Chemical, Materials and Biomolecular Sciences
ISSN: 2415-6620
Vol:9, No:10, 2015

Fiber Optic Sensors for Hydrogen Peroxide Vapor Measurement

H. Akbari Khorami, P. Wild, N. Djilali

***Abstract*—**This paper reports on the response of a fiber-optic sensing probe to small concentrations of hydrogen peroxide (H_2O_2) vapor at room temperature.

H_2O_2 has extensive applications in industrial and medical environments. Conversely, H_2O_2 can be a health hazard by itself. For example, H_2O_2 induces cellular damage in human cells and its presence can be used to diagnose illnesses such as asthma and human breast cancer. Hence, development of reliable H_2O_2 sensor is of vital importance to detect and measure this species.

Ferric ferrocyanide, referred to as Prussian Blue (PB), was deposited on the tip of a multimode optical fiber through the single source precursor technique and served as an indicator of H_2O_2 in a spectroscopic manner. Sensing tests were performed in H_2O_2-H_2O vapor mixtures with different concentrations of H_2O_2.

The results of sensing tests show the sensor is able to detect H_2O_2 concentrations in the range of 50.6 ppm to 229.5 ppm. Furthermore, the sensor response to H_2O_2 concentrations is linear in a log-log scale with the adjacent R-square of 0.93. This sensing behavior allows us to detect and quantify the concentration of H_2O_2 in the vapor phase.

***Keywords*—**Chemical deposition, fiber-optic sensors, hydrogen peroxide vapor, prussian blue.

I. Introduction

HYDROGEN peroxide (H_2O_2) is used in a broad range of applications such as aseptic processing of food and pharmaceuticals, water treatment plants, and industrial effluents for decontamination and disinfection [1], [2]. On the other hand, excessive H_2O_2 is also a health hazard because it plays a leading role in a variety of damage mechanisms [3]. Therefore, detection and measurement of H_2O_2 concentrations both in liquid and vapor phases is crucial.

Conventional techniques to detect H_2O_2 comprise titrimetric, colorimetric, and gasometric methods which, in general, require complex equipment and time consuming sample preparation, or have poor selectivity and limits of detection. Electrochemical and spectroscopic techniques on the other hand are able to determine small concentrations of H_2O_2 and have good selectivity [4]–[8], with spectroscopic techniques being preferred for many biochemical and industrial applications because of their immunity to electromagnetic interference. Spectroscopic detection includes chemiluminescent [9], [10], fluorescent [11], [12], and absorptive [6], [13] techniques.

Recently, fiber-optic sensing probes based on Prussian blue (PB) have shown reliable response to H_2O_2 concentrations in a liquid phase [14], [15]. A PB-based fiber-optic sensing probe fabricated through the layer-by-layer electrostatic self-assembly (ESA) of PB has been used successfully to detect H_2O_2 in a vapor phase [16]. However, this device was not able to determine concentrations of H_2O_2 in the vapor phase. In this paper, detection and determination of H_2O_2 concentrations in a vapor phase using a fiber-optic sensing probe based on chemically deposited PB is demonstrated.

PB was chosen as an H_2O_2 indicator for the proposed fiber optic probe because of its sensitivity and selectivity toward H_2O_2 [6], [17]. PB is a ferric ferrocyanide with the basic face-centered cubic crystalline structure consisting of iron ions linked by the cyanide groups with two chemical forms $Fe_4^{III}[Fe^{II}(CN)_6]_3$ and $KFe^{III}Fe^{II}(CN)_6$ [18], [19]. These two chemical forms are commonly known as "insoluble" and "soluble", respectively [19]. Both insoluble and soluble forms of PB are highly insoluble ($K_{sp} = 10^{-40}$), the difference refers to the simplicity of potassium peptization [20]. Large metal cations and water molecules, as well as other small molecules like H_2O_2, can be accommodated in the open structure of PB [20]. Chemical reduction and oxidation of PB leads to Prussian white (PW) (potassium ferrous ferrocyanide) and Berlin green (BG) (ferric ferricyanide), with chemical formula $K_2Fe^{II}Fe^{II}(CN)_6$, and $Fe^{III}Fe^{III}(CN)_6$, respectively [18], [20].

The H_2O_2 detection mechanism in PB-based fiber-optic sensing probes relies on the redox reactions of PB and its reduced state, PW, and the measurement of corresponding changes of the optical properties of the compound. PB is reduced to PW in the presence of a strong reducing agent, such as ascorbic acid. The reverse reaction happens when PW is exposed to a strong oxidizing agent, such as H_2O_2 resulting in PB. PB has a strong intervalence charge transfer absorption band near 700 nm because transition from $Fe^{III}Fe^{II}$ to $Fe^{II}Fe^{III}$ states. On the other hand, transparent PW has no distinct bands in the visible range of its absorption spectrum [21]. As a result, the increasing absorbance in the visible range while PW is oxidizing to PB by H_2O_2 can be used to detect the presence of this oxidant. Moreover, the initial PW state can be recovered by exposing PB to ascorbic acid.

H. Akbari Khorami is with the Institute for Integrated Energy Systems (IESVic) and Department of Mechanical Engineering, University of Victoria, Victoria, BC V8P5C2 Canada (Phone: 250-472-4221; e-mail: hakbarik@uvic.ca).

P. Wild is with the Institute for Integrated Energy Systems (IESVic) and Department of Mechanical Engineering, University of Victoria, Victoria, BC V8P5C2 Canada (Phone: 250-721-8901; e-mail: pwild@uvic.ca).

N. Djilali is with the Institute for Integrated Energy Systems (IESVic) and Department of Mechanical Engineering, University of Victoria, Victoria, BC V8P5C2 Canada (Phone: 250-721-6034; e-mail: ndjilali@uvic.ca).

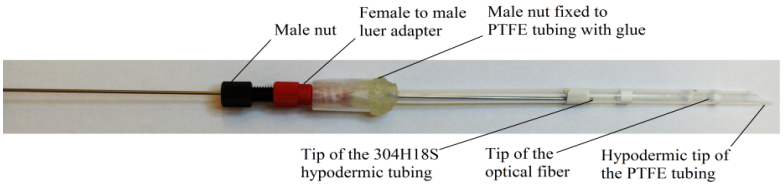

Fig. 1 PB-based fiber-optic sensing probe

II. Experimental Procedure

A. Materials

Potassium hexacyanoferrate (III) (or potassium ferricyanide) was used in an aqueous solution of 0.1 M hydrochloric acid (HCl) for synthesizing PB through a chemical process. L-ascorbic acid was used as the reducing agent for the PB to PW reaction. Sodium phosphate dibasic and potassium dihydrogen phosphate were used to prepare phosphate buffer solution (PBS) at pH 2 in which ascorbic acid solutions were prepared. H_2O_2 (30 wt%) and distilled water (18.2 MΩ cm) were used to prepare solutions for generating H_2O_2-H_2O vapor phase. All chemicals were used as received. The sources of the chemicals are documented in Table I.

TABLE I
Source of Chemicals

Chemicals	Product No.	Source
Potassium ferricyanide	13746-66-2	Sigma-Aldrich
L-ascorbic acid	25,556-4	Aldrich
Sodium phosphate dibasic	7558-79-4	EM science
Potassium dihydrogen phosphate	7778-77-9	Caledon
Hydrogen peroxide	4060-1-05	Caledon

B. Sensor Fabrication

The PB-based fiber-optic sensor was prepared using chemical deposition of a PB film onto the tip of a multimode optical fiber. As reported in our previous work [14], 10 mM of potassium ferricyanide, as a single source precursor, was added to 25 mL of an aqueous solution of 0.1 M HCl. The optical fiber was immersed in this prepared mix, and was kept at 40°C under continuous stirring at 300 rpm for 10 hours. The synthesis process was performed with exposure to fluorescent lamp light. Finally, the optical fiber was left in the solution to cool to room temperature. The prepared fiber-optic sensor was then removed from the solution and left at room temperature for one day. The sensor was then annealed at 100 °C for 15 min.

The PB-based fiber-optic sensor was integrated into a sensing probe for testing in H_2O_2 vapor. A short length of PTFE tubing was cut diagonally to form a hypodermic needle, and the other side of the PTFE tubing was positioned and fixed into a male nut using glue. The PB-based sensor was passed through the 304H18S hypodermic tubing such that the tip of the fiber was positioned beyond the distal tip of the hypodermic tubing. The 304H18S hypodermic tubing with the optical fiber was passed through a male nut, flangeless ferrule, and female to male Luer adapter to seal the sensing probe. Then, the sensing probe was assembled by connecting the 304H18S hypodermic tubing and PTFE tubing using the adapter and fixed nut, as shown in Fig. 1.

Using this sensing probe, it is possible to withdraw the fiber-optic sensor into the PTFE tubing to protect the tip of the fiber from damage when the fiber is passing through a parafilm membrane into the flask containing the H_2O_2-H_2O vapor. The sensor position can be adjusted to extend beyond the PTFE tubing when the fiber is immersed in ascorbic acid solution. The sensing probe is sealed before every sensing measurement by tightening the male nut.

C. Sensing Test and Instrumentation

Sensing tests were performed by alternately exposing the sensing probe to an ascorbic acid solution and H_2O_2-H_2O vapor, for recovery and oxidation steps of the PB/PW system. Fig. 2 illustrates the experimental setup. During the sensing test the light is generated by a white light source (Dunedin, FL LS-1, OceanOptics), is carried through the arm 1 (i.e. the common arm) and arm 1 to the tip of the fiber-optic sensor. Part of the scattered light from the PB/PW film on the tip of the fiber is collected by the optical fiber and guided back through the common arm and arm 2 into an optical fiber spectrometer (USB2000, OceanOptics), which measures the intensity of the light in a wavelength range of 370 to 1048 nm. The reflected spectrum was sampled at a frequency rate of 1 Hz using the software Spectra- Suite (OceanOptics, Dunedin, FL). The integrated values of intensity over the full range of the spectrometer (i.e. 370 to 1048 nm) were evaluated to study the response of the PB/PW system during both the oxidizing and the reducing steps.

H_2O_2 and H_2O were mixed in the Erlenmeyer flask with different weight ratios to generate different concentrations of H_2O_2 in the vapor phase. The mouth of Erlenmeyer flask was sealed with 2 sheets of parafilm. The tested concentrations of H_2O_2 in liquid and vapor phases are given in Table II [16].

TABLE II
H_2O_2 Concentrations in Liquid and Gas Phases [16]

Concentration in liquid phase (H_2O_2 wt%)	Concentration in vapor phase (H_2O_2 ppm)
20	229.5
15	164.6
10	105.2
5	50.6

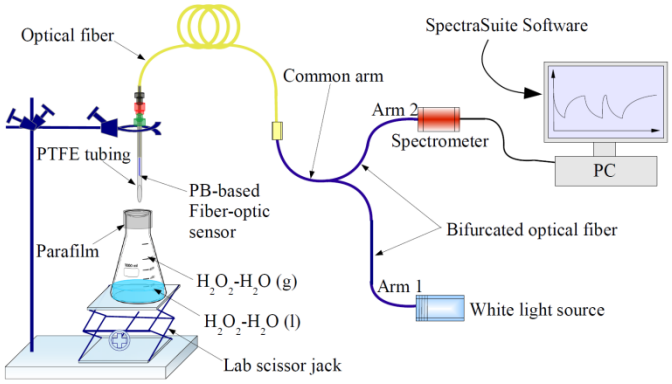

Fig. 2 Experimental setup

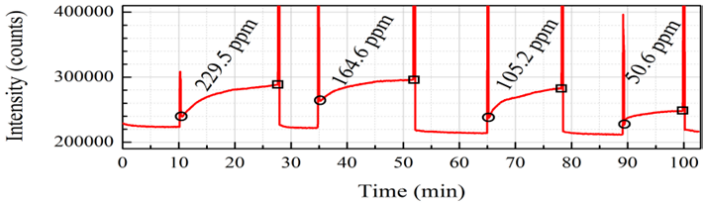

Fig. 3 Intensity response of the sensing probe to H_2O_2-H_2O vapor with different concentrations of H_2O_2

III. Calculation of H_2O_2 Vapor Concentration

To calculate the concentration of H_2O_2 in a H_2O_2-H_2O vapor mixture in equilibrium with H_2O_2-H_2O liquid mixture, the partial vapor pressure of H_2O_2 needs first to be determined. The partial vapor pressure of each component of an ideal mixture of liquids may be calculated using Raoult's law (1).

$$P_i = P_i^* X_i \tag{1}$$

where: P_i is the partial vapor pressure of component *i* in the liquid mixture, P_i^* is the vapor pressure of the pure component *i*, and X_i is the mole fraction of component *i* in the liquid mixture. However, the H_2O_2-H_2O system does not obey Raoult's law because the hydrogen bonding and interaction of the molecules with each other cause a system far from the ideal mixture. In this case, the activity coefficient of the component, γ_i, has to be inserted into Raoult's law (2):

$$P_i = P_i^* \gamma_i X_i \tag{2}$$

Partial vapor pressure of pure H_2O_2 and H_2O can be calculated from (3) and (4), respectively [22].

$$\log_{10} P^*_{H_2O_2} = 24.8436 - 3511.54/T - 4.61453 \log_{10} T - 3.60245\times10^{-3}T - 7.73423\times10^{-6}T^2 + 1.78355\times10^{-8}T^3 - 2.27008\times10^{-13}T^4 \tag{3}$$

$$\log_{10} P^*_{H_2O} = 19.389127 - 2861.9133/T - 3.2418662 \log_{10} T - 1.0799994\times10^{-4}T - 7.9189289\times10^{-6}T^2 + 1.5411774\times10^{-8}T^3 - 8.1926991\times10^{-12}T^4 \tag{4}$$

Also, the activity coefficient of H_2O_2 and H_2O can be calculated from (5) and (6), respectively [23].

$$\ln(\gamma_{H_2O_2}) = \frac{x^2_{H_2O}}{R.T}\left(\begin{matrix} B_0 + B_1.(3-4.X_{H_2O}) + B_2(1-2.X_{H_2O}).(5-6.X_{H_2O}) \\ + B_3.(1-2X_{H_2O})^2.(7-8X_{H_2O}) \end{matrix}\right) \tag{5}$$

$$\ln(\gamma_{H_2O}) = \frac{(1-x_{H_2O})^2}{R.T}\left(\begin{matrix} B_0 + B_1.(1-4.X_{H_2O}) + B_2(1-2.X_{H_2O}).(1-6.X_{H_2O}) \\ + B_3.(1-2X_{H_2O})^2.(1-8X_{H_2O}) \end{matrix}\right) \tag{6}$$

where: B_0, B_1, B_2, B_3 are functions of temperature [16], [23], R is the universal gas constant, and T is the absolute temperature.

Assuming the H_2O_2-H_2O vapor mixture is an ideal gas, the concentration of H_2O_2 in the vapor mixture may then be calculated using Dalton's law (7) and the Ideal gas law (8).

$$P_i = y_i P_t \tag{7}$$

$$P_t = \frac{n_t R T}{V_t} \tag{8}$$

where: P_i can be calculated by combining (2), (3), and (5), y_i is the mole fraction of the component *i* in the vapor mixture, n_t is the total amount of the vapor in mole, and V_t is the total volume of the vapor mixture.

By inserting (8) into the (7) and replacing y_i by its equivalent term, (n_i/n_t), the H_2O_2 concentration can be obtained as (9), in which MW_{H2O2} is the molecular weight of H_2O_2.

$$C_{H_2O_2} = \frac{P_{H_2O_2} MW_{H_2O_2}}{RT} \quad (9)$$

IV. Results and Discussion

The intensity of the reflected light from the distal end of the sensing probe during its exposure to H_2O_2-H_2O vapor at different concentrations of H_2O_2 is shown in Fig. 3. The circles and squares indicate the instant at which the sensing probe was exposed to H_2O_2-H_2O vapor and ascorbic acid, respectively. The intensity of the reflected light starts rising after the exposure of the sensing probe to H_2O_2-H_2O vapor due to oxidation of PW to PB. Following the immersion of the sensing probe in ascorbic acid, the intensity decreases as the ascorbic acid reduces the PB to PW.

The intensity response of each individual test was brought to the origin of the time axis at the moment of exposure to H_2O_2-H_2O vapor, and an inverse exponential curve fitted to the data, as shown in Fig. 4. For each concentration, the characteristic response time (τ) (i.e. the time elapsed for the signal to reach 63% of the intensity of the plateau state) was extracted from the inverse exponential curve and plotted in Fig. 5. This plot shows that the probe exhibits a linear response to H_2O_2 concentration on a log-log scale. This linear behavior suggests that this sensing probe can be used not only to detect the presence of H_2O_2 vapor but also to quantify the concentration of H_2O_2 in the vapor phase.

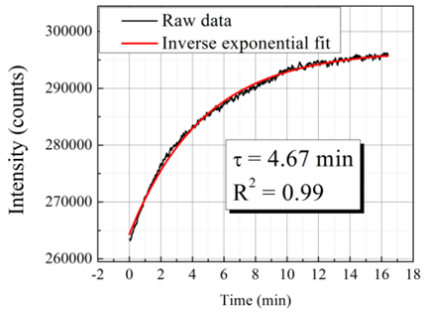

Fig. 4 Intensity response to 164.6 ppm H_2O_2

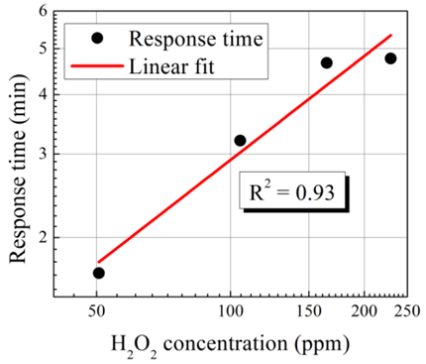

Fig. 5 Time response versus H_2O_2 concentration

V. Conclusion

Detection and measurement of small concentrations of H_2O_2 in the vapor phase has been demonstrated. The sensor shows a linear response to the H_2O_2 concentration on a log-log scale with the adjacent R-square of 0.93. The sensor features fast and reliable responses and is suitable to be used in industrial applications.

Acknowledgment

The authors gratefully acknowledge funding provided by the Natural Sciences and Engineering Research Council of Canada (NSERC).

References

[1] P. B. L. Chang, T. M. Young, "Kinetics of methyl tert-butyl ether degradation and by-product formation during UV/hydrogen peroxide water treatment," *Water Research*, vol. 34, no. 8, pp. 2233-2240, 2000.
[2] B. A. H. von Bockelmann, I. L. I. von Bockelmann, "Aseptic packaging of liquid food products: a literature review," *J. Agric. Food Chem.*, Vol. 34, pp. 384-392, 1986.
[3] Y. J. Byun, S. K. Kim, Y. M. Kim, G. T. Chae, S. W. Jeong, S. B. Lee, "Hydrogen peroxide induces autophagic cell death in C6 glioma cells via BNIP3-mediated suppression of the mTOR pathway," *Neuroscience Letters*, vol. 461, pp. 131-135, 2009.
[4] J.Y. Zheng, Y. Yan, X. Wang, W. Shi, H. Ma, Y.S. Zhao, J. Yao, "Hydrogen peroxide vapor sensing with organic core/sheath nanowire optical waveguides," *Advanced Materials*, vol. 24, pp. OP194-OP199, 2012.
[5] R. Koncki, T. Lenarczuk, A. Radomska, S. Glab, "Optical biosensors based on prussian blue films," *Analyst*, vol. 126, pp. 1080-1085, 2001.
[6] I. DelVillar, I.R. Matías, F.J. Arregui, R.O. Claus, "ESA-based in-fiber nanocavity for hydrogen-peroxide detection," *IEEE Transactions on Nanotechnology*, vol. 4, pp. 187-193, 2005.
[7] L. Wang, H. Zhu, Y. Song, L. Liu, Z. He, L. Wan, S. Chen, Y. Xiang, S. Chen, J. Chen, "Architecture of poly (o-phenylenediamine)–ag nanoparticle composites for a hydrogen peroxide sensor," *Electrochimica Acta*, vol. 60, pp. 314-320, 2012.
[8] Q. Yan, Z. Wang, J. Zhang, H. Peng, X. Chen, H. Hou, C. Liu, "Nickel hydroxide modified silicon nanowires electrode for hydrogen peroxide sensor applications," *Electrochimica Acta*, vol. 61, pp. 148-153, 2012.
[9] T.M. Freeman, W.R. Seitz, "Chemiluminescence fiber optic probe for hydrogen peroxide based on the luminol reaction," *Analytical Chemistry*, vol. 50, pp. 1242-1246, 1978.
[10] A. Tahirovic, A. Copra, E. Omanovic-Miklicanin, K. Kalcher, "A chemiluminescence sensor for the determination of hydrogen peroxide," *Talanta*, vol. 72, pp. 1378-1385, 2007.
[11] E.W. Miller, O. Tulyathan, E.Y. Isacoff, C.J. Chang, "Molecular imaging of hydrogen peroxide produced for cell signaling," *Nature chemical biology*, vol. 3, pp. 263-267, 2007.
[12] E.W. Miller, A.E. Albers, A. Pralle, E.Y. Isacoff, C.J. Chang, "Boronate-based fluorescent probes for imaging cellular hydrogen peroxide," *Journal of the American Chemical Society*, vol. 127, pp. 16652-16659, 2005.
[13] C. Tagad, S. Dugasani, R. Aiyer, S. Park, A. Kulkarni, S. Sabharwal, "Green synthesis of silver nanoparticles and their application for the development of optical fiber based hydrogen peroxide sensor," *Sensors and Actuators B: Chemical*, vol. 183, pp. 144-149, 2013.
[14] H. Akbari Khorami, J. F. Botero-Cadavid, P. Wild, N. Djilali, "Spectroscopic detection of Hydrogen peroxide with an optical fiber probe using chemically deposited Prussian blue," *Electrochimica Acta*, vol. 115, pp. 416-424, 2014.
[15] J. F. Botero-Cadavid, A. G. Brolo, P. Wild, N. Djilali, "Detection of hydrogen peroxide using an optical fiber-based sensing probe," *Sensors and Actuators B: Chemical*, vol. 185, pp. 166-173, 2013.
[16] J. F. Botero-Cadavid, "Fiber-optic sensor for detection of hydrogen peroxide in PEM fuel cells," PhD dissertation, University of Victoria, 2014, Appendix D, pp. 184- 206.
[17] R. Koncki, O.S. Wolfbeis, "Composite films of prussian blue and n-substituted polypyrroles: Fabrication and application to optical

determination of ph," *Analytical Chemistry*, vol. 70, pp. 2544-2550, 1998.
[18] K. Itaya, T. Ataka, S. Toshima, "Spectroelectrochemistry and electrochemical preparation method of prussian blue modified electrodes," *Journal of the American Chemical Society*, vol. 104, pp. 4767-4772, 1982.
[19] V.D. Neff, "Electrochemical oxidation and reduction of thin films of Prussian blue," *Journal of the Electrochemical Society*, vol. 125, pp. 886-887, 1978.
[20] D. Ellis, M. Eckhoff, V. Neff, "Electrochromism in the mixed-valence hexacyanides. 1. voltammetric and spectral studies of the oxidation and reduction of thin films of prussian blue," *The Journal of Physical Chemistry*, vol. 85, pp. 1225-1231, 1981.
[21] R. Koncki, "Chemical sensors and biosensors based on Prussian blues," *Critical Reviews in Analytical Chemistry*, vol. 32, no. 1, pp. 79-96, 2002.
[22] S. L. Mannat, M. R. R. Mannat, "On the analysis of mixture vapor pressure data: The hydrogen peroxide/ water system and its excess thermodynamic functions," *Chemistry: A European Journal*, vol. 10, pp. 6540–6557, 2004.
[23] S. Radl, S. Ortner, R. Sungkorn, J. G. Khinast, "The engineering of hydrogen peroxide decontamination systems," *Journal of Pharmaceutical Innovations*, vol. 4, pp. 51–62, 2009.